INSTITUTE OF PHYSICS PUBLISHING JOURNAL OF OPTICS A: PURE AND APPLIED OPTICS

J. Opt. A: Pure Appl. Opt. **6** (2004) 491–503 PII: S1464-4258(04)70555-3

The double superficiality of the frontal image of the Turin Shroud

Giulio Fanti and Roberto Maggiolo

Dipartimento di Ingegneria Meccanica, Università di Padova, Via Venezia 1, 35137 Padova, Italy

E-mail: giulio.fanti@unipd.it

Received 13 October 2003, accepted for publication 12 March 2004
Published 13 April 2004
Online at stacks.iop.org/JOptA/6/491
DOI: 10.1088/1464-4258/6/6/001

Abstract
Photographs of the back surface of the Turin Shroud were analysed to verify the existence of a double body image of a man. The body image is very faint and the background not uniform; i.e., the signal-to-noise ratio is lower than one. Therefore, image processing, developed ad hoc, was necessary to highlight body features. This was based on convolution with Gaussian filters, summation of images, and filtering in spatial frequency by direct and inverse bidimensional Fourier transformations. Body features were identified by template matching. The face and probably also the hands are visible on the back of the Turin Shroud, but not features related to the dorsal image.

Keywords: image processing, very low signal-to-noise ratio, fast Fourier transform, convolution, Turin Shroud

List of acronyms

TS	=	Turin Shroud
fs	=	front surface of TS
bs	=	back surface of TS
FFT	=	fast Fourier transform
IFFT	=	inverse fast Fourier transform
IR	=	infrared
UV	=	ultraviolet

1. Introduction

The Turin Shroud (TS) is 4.4 m long and 1.1 m wide; on it the complete frontal and dorsal images of the body of a man are indelibly impressed (figure 1). It has one frontal and one dorsal image of a naked man, separated by a space between the two images of the head. The images show an adult male, well proportioned and muscular, with beard, moustache, and long hair, and are compatible with a man 175 ± 2 cm tall enveloped in a sheet (Basso *et al* 2002).

The TS is believed by many to be the burial cloth in which Jesus of Nazareth was wrapped before being placed in a tomb in Palestine about 2000 years ago. The TS cloth is hand-woven, each thread (non-constant diameter of about 0.25 mm) is composed of 70–120 linen fibres (Fanti and Moroni 2002), and it has a herringbone 3/1 weft. Impressed on the cloth are many other marks due to blood, fire, water, and folding, which have greatly damaged the double body image.

After restoration of the TS by the nuns in Chambéry, following the 1532 fire which had seriously damaged it, a piece of Holland cloth was sewn to the back of the TS. The points at which the two pieces of cloth were put together prevented observation of the back surface of the TS until 2000, when the central part was unstitched to allow the passage of a scanner. Images of the back surface of the TS corresponding to the frontal and dorsal images could thus be acquired. In 2002, the TS was completely unstitched from the Holland cloth and its back surface was photographed (Ghiberti 2002), both overall and in detail. Lastly, a new reinforcing cloth, which again now prevents direct observation of the back of the TS, was sewn in place.

In 1931, Enrie (1933) photographed the TS at high resolution using an orthochromatic plate. The TS body image appears as a photographic negative, and its luminance levels can be related to the 3D image of a human body. Some other characteristics of the body image (Jackson 1990, Moran and Fanti 2002) are: superficiality, resolution of some millimetres, and absence of side images. The image is chemically due to molecular changes in the linen fibres of the cloth and it is

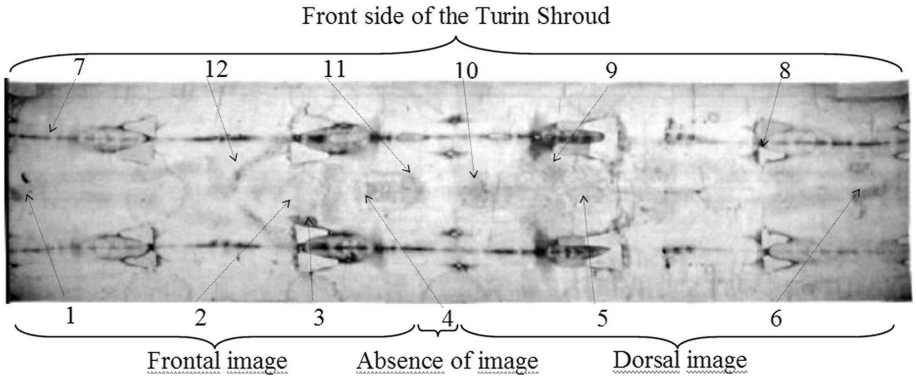

Figure 1. The body image and marks visible on the TS. (1) A wound in the right foot. (2) Marks of water. (3) A wound in the side. (4) Folds in the cloth. (5) Marks of scourging. (6) The heel and sole of the right foot. (7) Carbonized lines in the cloth, due to the fire of 1532. (8) Mending done by Chambéry nuns after the fire of 1532. (9) Bruises due to transport of the patibulum. (10) Wounds on the head, consistent with the effects of a 'crown of thorns'. (11) A wound on the forehead. (12) A wound in the left wrist.

consistent with the vertical projection of a human body. The image (dehydration and oxidation of cellulose) is present only on the outer surface of the linen fibres (their medullas are not coloured). There are no signs of cementation among the fibres and the maximum luminance level of the frontal image is the same as that of the dorsal image; the luminance level of the face is about 20% higher.

The possible presence of an image on the back of the TS, as postulated by Jackson (1990), is important for understanding the mechanism of formation of the body image. The image superficiality is very influential on the results of this paper and it is supported by a lot of statements (Weaver 1980, Pellicori and Evans 1981, Schwalbe and Rogers 1982, Jumper *et al* 1984); for example Adler (1999) writes: '*The image only goes one fiber deep, lying on top of the crowns of the threads of the weave of the cloth*' and Jackson *et al* (1984) specifies that, comparing the reflected light photograph with the equivalent transmitted light photograph, the intensity of the body image appears to be considerably less than for those same areas in the reflected light image; thus the much fainter body image in the transmission image is explainable as a discoloration residing only on the uppermost surface fibres of the cloth. Furthermore Rogers (2003) states that he observed the area of the body image near the nose, and that the image only involved the outermost linen fibres, for a maximum thickness of about 0.03 mm.

When dealing with the TS, we define fs (front surface) images as referring to the visible side of the sheet, i.e., the surface always shown during exhibition; we define bs (back surface) images as referring to the surface normally hidden by a reinforcement cloth sewn onto the back of the TS. On the basis of the image of the face acquired by scanning (Archdiocese 2000), it was presumed that a very faint image appears on the bs of the TS (Moran and Fanti 2002). The photographs of the bs taken in 2002 (Ghiberti 2002) show that some traces of hair on the fs are visible to the naked eye. Ghiberti proposes that perhaps the hair too left an image on the bs, because organic matter from it, such as sebum, would penetrate the fabric, but this hypothesis must be rejected, because sebaceous materials would be fluorescent under ultraviolet light, and the UV photographs taken by Miller and Pellicori (1981) in 1978 of the fs of the TS do not show any fluorescence near the hair.

In this work, some photos of the bs of the TS are analysed by eidomatic procedures, in order to verify whether and where there is a body image on the back of the sheet and whether it corresponds in both position and form to the front one (Maggiolo 2002/2003). Unfortunately, the original photographs of the bs, owned by the Archdiocese of Turin, have not yet been made available to the scientific world. The only photographs available for analysis are those published by Ghiberti (2002) and the results of scanning (Archdiocese 2000). They were made available to the present authors for scanning and image processing, thanks to kind authorization by Ghiberti, of the Archdiocese of Turin.

The ad hoc eidomatic procedure, used to highlight details in photographs not visible to the naked eye, was first applied to the photograph of the face taken by Enrie (1933) in 1931, to compare the effectiveness of the method. The procedure was then applied to various images of the face, on both the fs and bs of the TS, in visible and IR light, and to photographs of the arms and shoulders (fs and bs), for more detailed comparisons regarding the possible double superficiality of the body image.

The procedure was based on image convolution and subsequent filtering in the spatial frequency domain using Fourier transforms. Other work based on Fourier transforms (Marion 1998) has been proposed to enhance some details of the TS, but ours is quite different, because it is suitable for enhancing body details partially masked by bands of colour.

2. Optical characteristics of images and conventions

The following conventions for the black-and-white images of the TS must now be established. The body image has some characteristics of a photographic negative because the protruding parts are darker in tone than the rest of the body: the luminance distribution is opposite to that which we perceive in reality. For better perception of anatomical details, the photographs are presented in negative with respect to the originals; that is, the luminance levels are inverted.

The frontal body image of the TS is a mirror image of the man: the photographs are therefore specular with respect to the original image. As an example for clarification, let us consider the bloodstain in the centre of the forehead, due to a wound to the frontal vein, which has a typical 'ε' shape, since it follows the course of the wrinkles of the face. This ε-shaped stain is used as a reference in the photographs, but is always shown inverted, like a number '3' (figure 2).

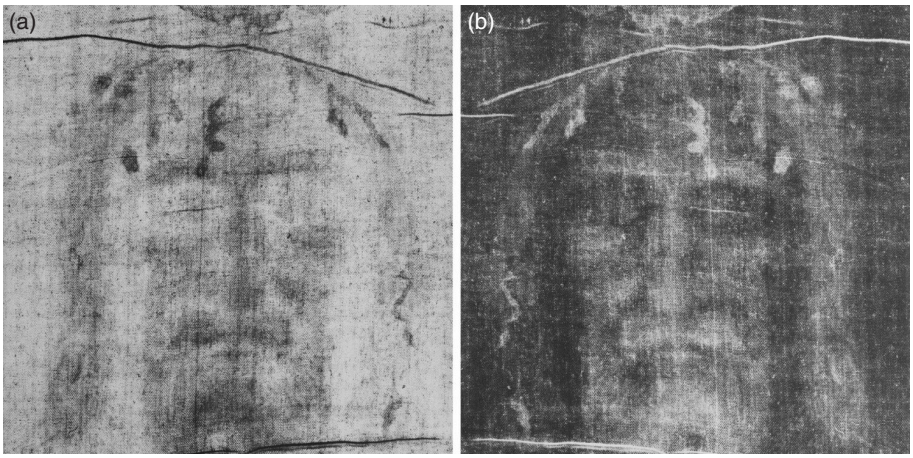

Figure 2. (a) The image of the face of a man, on the fs of the TS, as it appears to observers. The characteristic ε-shaped bloodstain on the front is shown for reference. (b) The mirror image of (a), with inverted luminance levels. The reference bloodstain takes on the shape of the number 3.

The photos of the bs of the TS are not specular, in order to simplify comparisons with the corresponding ones on the fs. Therefore, the bloodstain on the forehead is still in the form of a '3' rather than an 'ε'. The hand images were produced on the basis of the same criterion.

The cloth shows bands of yarn of slightly different colours, as the various batches of thread used to weave the cloth show varying degrees of decay. The yellowness of the TS has been defined in the UV–visible range (Gilbert and Gilbert 1980).

The body image is very faint: reflected luminances (or optical densities) are typically less than 10% in the visible range (Schwalbe and Rogers 1982, Jumper *et al* 1984). For example, if a non-contrast-enhanced photograph is digitized to 256 luminance levels (Schwortz (1982) colour photograph of 1978), the mean b/w luminance level of the background near the face is 210, and a darker mean level of 191 is found near the nose and eyebrows; mean values are obtained in windows 10 mm × 10 mm wide. This implies that contrast enhancement is necessary for the human eye–brain system to perceive body features well.

This type of enhancement also evidences other details such as the herringbone weft of the cloth, its longitudinal bands, water stains, bloodstains, and other defects which can all be reduced by means of proper digital image processing.

The bs of the TS shows that the body image, if it exists, is fainter than that on the fs and is partially hidden by the longitudinal bands. If a non-contrast-enhanced photograph is digitized into 256 luminance levels (Ghiberti 2002), the mean b/w luminance level of the background near the face is 197, corresponding to a bright band, and 179 in the dark band. This means that there is a variation of about 10% in luminance levels, due to the presence of the bands. A darker mean level of 170 is found near both nose and hair—this means that there is a variation of only about 5% in mean luminance level between a dark band and the maximum value of a body feature. In other words, the signal-to-noise ratio is about 0.5; i.e., some image processing is needed to make the body features perceptible to the human eye–brain system.

As regards the spectral characteristics of the images, the face photographed by Enrie (1933) (fs), using an orthochromatic plate of 30 cm × 40 cm, is analysed here as a reference, because it is still the photograph which shows the best contrast available to researchers. This photograph was digitized by means of square pixels of $L_p = 0.102 \pm 0.001$ mm, corresponding to a spatial sampling frequency f_s of

$$f_s = 1/L_p = 9800 \pm 100 \text{ m}^{-1}. \quad (1)$$

The fast Fourier transform (FFT) of the Enrie photograph, in a 2048 × 2048 window, has an upper frequency f_u of

$$f_s/2 = 4900 \pm 50 \text{ m}^{-1}, \quad (2)$$

and a frequency resolution f_r of

$$f_r = f_s/2048 = 4.78 \pm 0.05 \text{ m}^{-1}. \quad (3)$$

Figure 3 shows the FFT of the photograph of figure 2(b). The body image has a resolution of a few millimetres because the body contours are faded and no details below this limit are discernible. The corresponding spatial frequencies are therefore less than 100 m^{-1}—much smaller than those characterizing other noise due, for example, to the weft, sized at about 1.0 and 1.6 mm along the horizontal and vertical directions respectively, with typical spatial frequencies of 980 and 630 m^{-1}. Accordingly, the pixels representing the body image values in the FFT plot are only located around its centre. It is therefore clear that low-pass frequency filtering, with spatial cut-off frequencies of about 100 m^{-1}, can eliminate image noise such as that of the weft, leaving the body characteristics of the image unchanged.

To determine the body image resolution more accurately, the following inverse method was employed. All luminance levels belonging to a predefined radius centred at the zero-frequency value of the FFT of the body image were set at zero, and an inverse FFT (IFFT) was then obtained. The resulting image corresponds to the initial photograph, but without its lower spatial frequencies and therefore without its body characteristics.

In figure 4, a radius of 13 pixels from the centre was selected, and all frequencies below the cut-off frequency f_c were then eliminated:

$$f_s = nf_r = 62.1 \pm 0.6 \text{ m}^{-1}. \quad (4)$$

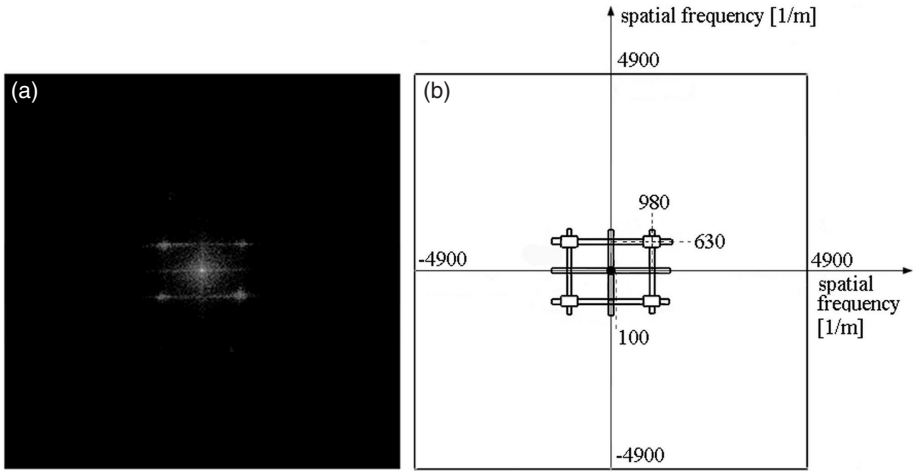

Figure 3. (a) The bidimensional Fourier transform (power spectrum) of the image shown in figure 2(b). Clearer spatial frequency peaks are evidenced on the black background. (b) A sketch of the plot shown in figure 3(a): frequency peaks at 980, 630 m^{-1} correspond to the weft of the fabric and frequencies of body features are limited to a circle of radius 100 m^{-1}.

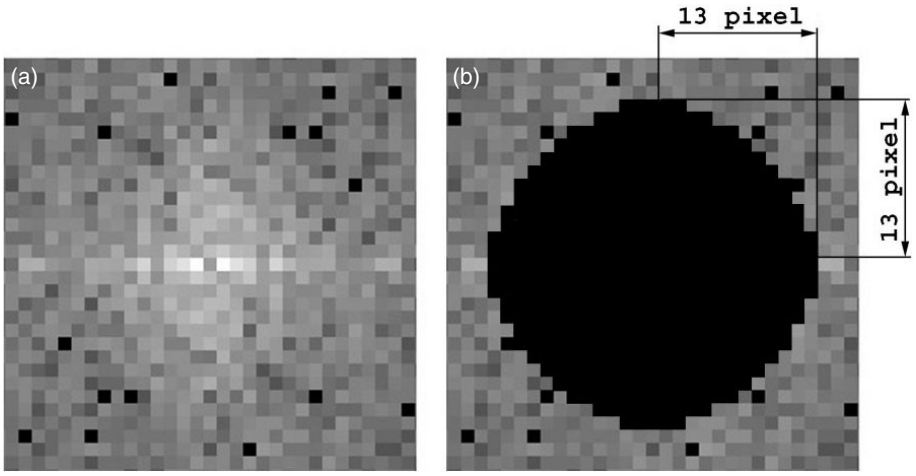

Figure 4. (a) A magnification of the central part of figure 3(a). Each pixel corresponds to a resolution in spatial frequency of $f_r = 4.78 \pm 0.05$ m^{-1}. (b) The luminance values are set at zero (black) in all pixels with spatial frequency below 62.1 ± 0.6 m^{-1}.

This procedure was repeated for radii of 17 and 21 pixels, yielding respectively spatial cut-off frequencies of $f_s = 81.2 \pm 0.8$ and 100.4 ± 1.0 m^{-1}. Figure 5 shows the IFFT of the Enrie face after frequency filtering. Clearly, details of the lips disappear (figure 5(c)), showing that the body features are characterized by frequencies greater than 80 m^{-1} but less than 100 m^{-1}—i.e., details with a spatial period of about 10 mm and therefore a resolution of about 5 mm.

3. Digital image processing

A technique of digital image processing able to evidence the body features present in an image which contains noise of various types with signal-to-noise ratios of less than one is presented and discussed here. This technique, using Optimas 6.1® and Photoshop 7.0® software, covers several phases:

(1) acquisition of printed images, by scanning and digital processing;
(2) processing to eliminate the vertical band effect in the background;
(3) processing to eliminate the narrow marks of folds, etc;
(4) choice of suitable windows, filtering in spatial frequency in them, and reduction of noise caused by the windows;
(5) processing to render the background more uniform, and image enhancement.

3.1. Image acquisition and processing

The following images were acquired and processed:

(a) the face, fs, high-resolution photograph taken by Enrie (1933), with orthochromatic film;
(b) the face, fs and bs, obtained by means of a scanner positioned in contact with the TS, screened at 360 dpi (Archdiocese 2000)—this image, although of inferior quality in comparison with the images in (c), does serve for comparing results;
(c) faces, fs and bs, screened at 360 dpi (Ghiberti 2002);
(d) the face, fs, high-resolution photograph taken by Judica Cordiglia (1976) in 1969 with an infrared (IR) film;
(e) hands, fs and bs, screened at 360 dpi (Ghiberti 2002) to verify the possible presence of images in zones different from the frontal image on the back;

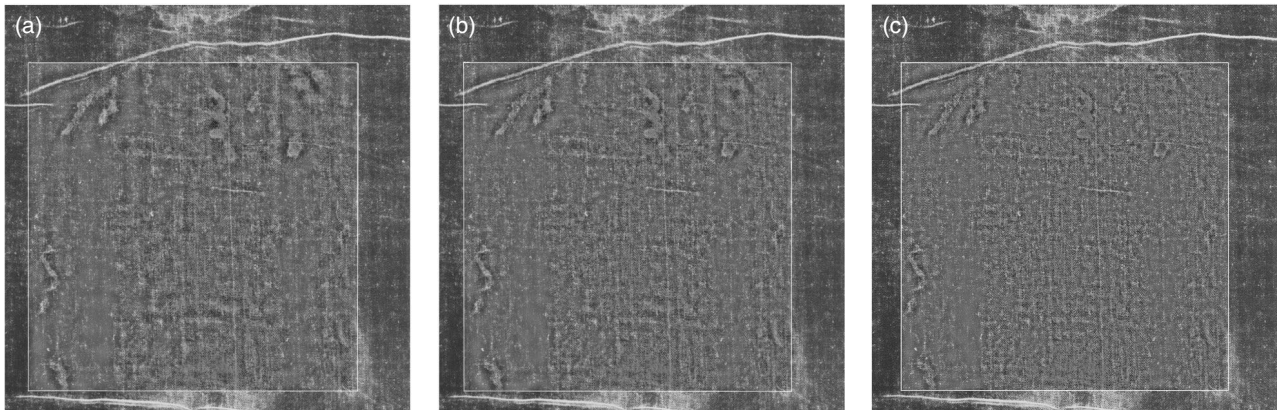

Figure 5. (a) The resulting IFFT of the image shown in figure 2(b), in which all frequencies lower than $62.1 \pm 0.6\ m^{-1}$ are eliminated. Many body features, although not the lips, are eliminated. ((b), (c)) The results after high-pass filtering of spatial frequencies lower than 81.2 ± 0.8 and $100.4 \pm 1.0\ m^{-1}$ respectively. In (c) the lip features are also cancelled.

(f) a photograph of the shoulders, bs, screened at 360 dpi (Ghiberti 2002) to verify the possible presence of images in zones of the bs image.

The processing procedure was developed to highlight further the body features of images (c), because these are perhaps the most delicate and interesting to study.

Other photographs not being available, the images of the bs of the TS were digitized from printed volumes, with reprint permission kindly furnished by Giuseppe Ghiberti (Archdiocese 2000, Ghiberti 2002).

For example, in the case of the face (Ghiberti 2002), the original image, colour printed with half-tone screening of 360 dpi, was acquired by scanning at a resolution of 600 dpi. Screening was subsequently removed, convoluting the digitized image with a Gaussian filter of radius 1.5 and then using a 3×3 matrix filter.

Image sizes were then reduced to 58%. An image matrix of 2100×2948 pixels was obtained for the whole image acquired from the bs of the TS; the dimensions of the face in the photograph (about 1800×2100 pixels) are about 130 mm $\times$ 150 mm and the size of a square pixel is 0.07 mm on the scale of the photograph. As the acquired image of the photograph is reduced to 66% of its real size, the real pixel size corresponds to about 0.10 mm. The digital photograph resolution of 0.10 mm is therefore good enough for highlighting body details of some millimetres.

3.2. Processing to eliminate the vertical band effect (background)

The TS has longitudinal bands of different colours, probably due to the process of retting, which disturb the body images, especially on the back, where there are the fewest variations in luminance. These bands introduce nearly the same luminance values in the longitudinal direction. To eliminate the bands and to make the background more uniform, the following matrix summation was performed.

Let us consider, as an example, the photograph of the arm zone, bs (figure 6(a)). This image was convoluted with a Gaussian filter of radius 100 pixels to eliminate all its higher frequencies; three samplings of horizontal lines were made in zones without bloodstains or body image, and their mean profiles were evaluated (figure 6(b)). The result was an image having dimensions equal to the initial ones and a profile of luminance levels, in the horizontal direction, opposite to those of the mean background but constant in the vertical direction (figure 6(c)). The resulting matrix (the sum of the images of figures 6(a) and (c) minus a constant luminance level of 30 to obtain the same mean luminance as for figure 6(a)) was taken to obtain the image shown in figure 6(d), in which the background is more uniform.

3.3. Processing to eliminate fold marks

The photographs show several marks, mainly straight, generally caused by folds in the fabric. As they do not always follow the same direction, processing unlike that described in section 3.2 was employed, to reduce or eliminate these marks. Frequency filtering in the spatial frequency domain was performed to reset the characteristic frequencies inside a pre-selected window with strong longitudinal development (for instance, 128×2048 pixels).

These windows were chosen in the image to entirely include the noise to be removed (represented by a narrow vertical fold in figure 7(a)). In fact, taking the FFT of this window (figures 7(b), (c)) practically introduces a single high luminance value corresponding to the spatial frequency of the thickness of the fold to be eliminated. This value was then set at zero and the IFFT was obtained (figure 7(d)). The defect is practically absent in the final image.

3.4. Spatial frequency filtering inside windows and noise reduction

Filtering was performed by a trial-and-error procedure, consisting of taking a direct FFT and step spatial frequency filtering, by resetting the luminance values of some frequencies and then obtaining the IFFT. If the resulting image did not introduce evident loss of information of body features, the procedure was repeated, resetting the values of the lower spatial frequencies in both horizontal and vertical directions. This procedure was continued until some frequency related to the body image was cancelled.

Sixteen windows were selected inside the image, in order to obtain spatial frequency filtering in an independent way.

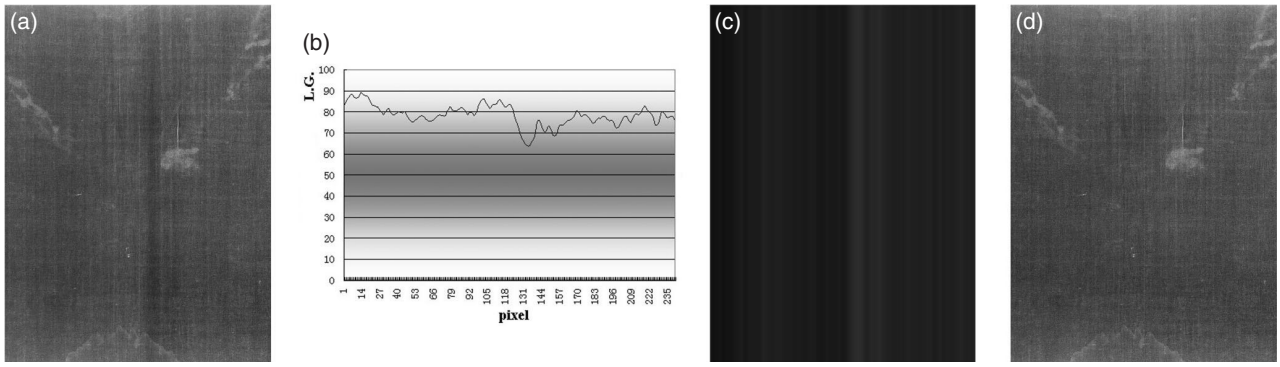

Figure 6. (a) An image of the hands, bs (Ghiberti 2002): a black vertical band is visible in the centre, a disturbance which interferes with the highlighting of the body. (b) Mean luminance profiles of three undisturbed horizontal pixel rows. (c) The compensation image. (d) The resulting image of the hands after summation of the images of (a) and (c): the black band is cancelled.

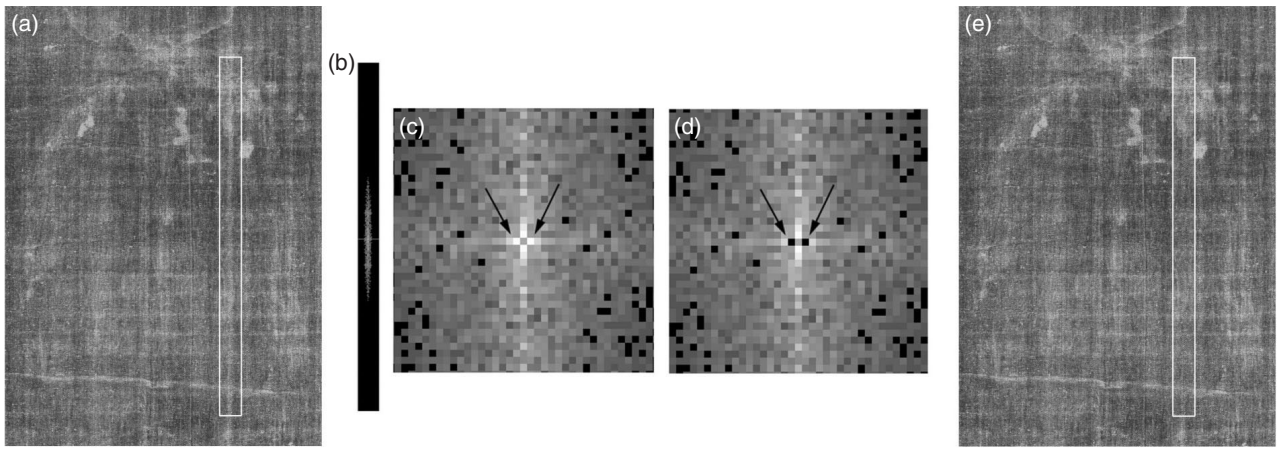

Figure 7. (a) The mark windowed in the face image, bs (Ghiberti 2002). (b) The FFT power spectrum for the window selected in (a). (c) A magnification of (b), corresponding to the central area. (d) Two luminance levels (arrow), reset (black) to eliminate a narrow segment. (e) The results of the processing.

Every adjacent window, of dimensions 512 × 512 pixels, was overlapped for a band of 12 pixels, to make their edges less evident during reconstruction of the final image. It should be noted that the spatial frequency resolution is four times better in the FFT spectrum of the whole image than in that of each window, and that the full-scale frequency remains the same.

Independent frequency filtering in each window was preferred, rather than direct processing of the whole image, for the following reason: the FFT of the whole image (i.e., the power spectrum), in terms of peak amplitudes, involves adding the various spatial frequencies of the characteristics of many body features present in the image. It is therefore easier to cancel a sinusoidal component (or spatial frequency) of a detail which does not correspond to the body in a certain zone of the image, but which is important in another zone. Filtering of the whole image may then be either less effective, or it may cancel a detail of interest. Instead, if filtering is performed inside a smaller window, each one yields better definition of the particular contour curve, in the x–y plane of the FFT power spectrum, relative to the cut-off filter. The information content of such simpler images is lower, and therefore easier to check.

For example, a comparison may be made between figure 8(a), which results from the procedure performed by filtering the whole photograph of the face acquired by Enrie (1933), and figure 8(b), which results from the procedure performed by means of 16 windows defined in the same image. Figures 8(c) and (d) correspond to the filtered power spectrum of one window (figure 8(b)).

Clearly, some details of the body image are lost in figure 8(a), and the result is a 'straightening' of the body features, due to excessive simplification of the image in terms of spatial frequency content.

The grid effect caused by image windowing was further reduced by double blurring of the zones corresponding to the grid. In particular, a first convolution in horizontal and vertical windows, 35 pixels wide, was performed with a Gaussian filter with a radius of 15 pixels (matrix size 31 × 31). A second convolution of the whole image was performed using a Gaussian filter with a radius of 20 pixels.

3.5. Processing to render the background more uniform, and image enhancement

As the background of the image does not always have a uniform luminance level, the FFT was obtained and the corresponding spatial frequency values reset, to yield a more uniform background. For instance, the photograph of the face, bs (Ghiberti 2002), has an upper zone which is darker. To make the background more uniform, the FFT was obtained inside a window of 2048 × 2048 pixels. The characteristic frequencies are relatively low and were found on the vertical

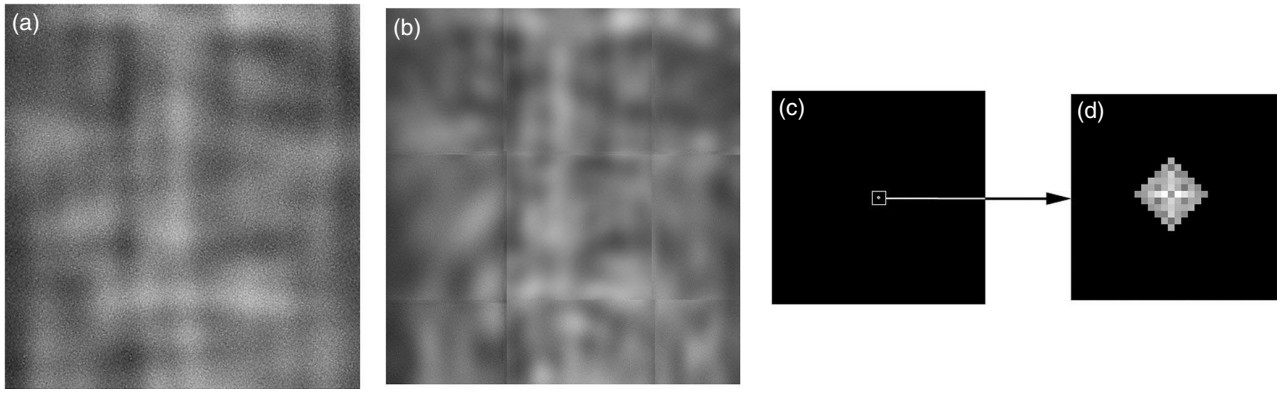

Figure 8. (a) A detail of the face, acquired by Enrie (1933), after FFT filtering of the whole image. (b) The same detail as in (a), filtered by means of windowing: the moustache appears clearly resolved and realistic. (c) The FFT of one of the windows of (b). (d) A magnification of the filtered zone (black) of (c).

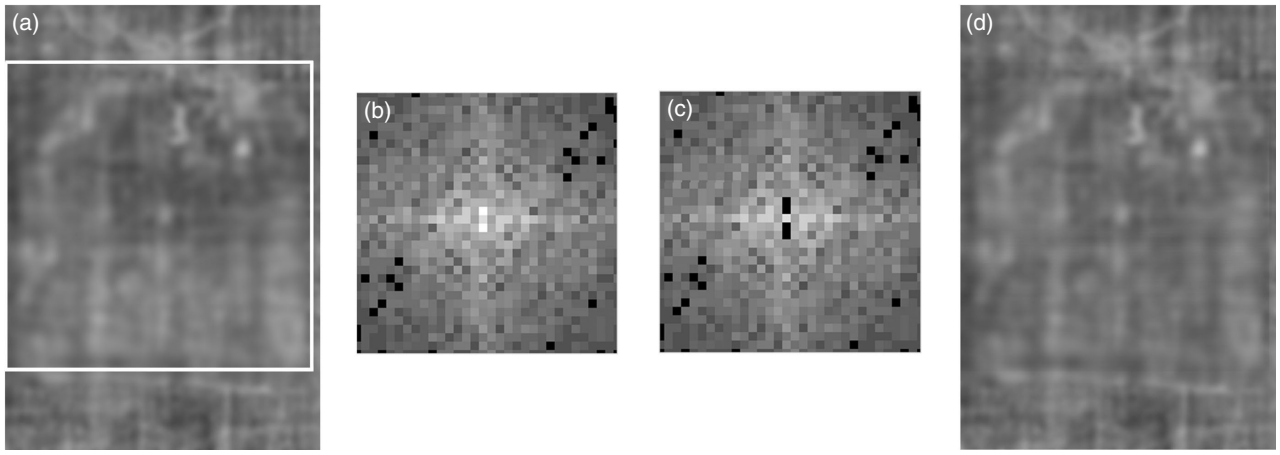

Figure 9. (a) A window processed in the photograph of the face, bs (Ghiberti 2002), showing an upper darker area. (b) A central magnification of the FFT power spectrum of (a). (c) The central pixel reset (arrows). (d) The resulting filtered image.

axis of the FFT. Once found, they were reset and the IFFT was obtained. Figures 9(a) and (b) show respectively the image and its FFT before processing, and figures 9(c) and (d) those after correction.

At the end of these operations, the resulting image has a variance in luminance values of less than 20. In this case, perception of details is not easy for the human eye, which can clearly distinguish about 60 different shades of grey. Image enhancement was therefore applied by gamma correction of the luminance values and equalization of the resulting histogram. Lastly, the dimensions of the images were reduced to 33%.

The results of the processing of some of the images analysed are presented in figures 10(a)–(d).

Figures 11(a) and (b) compare the face, bs and fs (Ghiberti 2002). Subjectively, some body features also appear on the bs, but objective analysis is presented in the following section.

4. Identification of shapes

As figures 11(a) and (b) show, the processed image of the face on the bs of the TS (Ghiberti 2002) highlights some body features which are similar to those on the front.

For an objective judgment of this comparison, template matching was carried out using eVision's EasyMatch 6.0® software thus allowing comparisons of details contained in images defined by square windows of dimensions up to 250 × 250 pixels. For this purpose, the image sizes were reduced to 35%. The software furnishes the score, the position of the window, its rotation, and its scale factor in comparison with the template.

The correlation formula used to compute the score S of a pattern at a given location is

$$S = \frac{\sigma_{\mathrm{IP}}}{\sqrt{\sigma_{\mathrm{II}}\sigma_{\mathrm{PP}}}} \tag{1}$$

where σ_{IP} is the covariance of the pixel value between the pattern and the part of the image used:

$$\sigma_{\mathrm{IP}} = \frac{1}{nm}\sum_{i=1}^{n}\sum_{j=1}^{m}(I_{i,j} - m_{\mathrm{I}})(P_{i,j} - m_{\mathrm{P}}). \tag{2}$$

σ_{PP} is the variance of the pixel value in the pattern:

$$\sigma_{\mathrm{PP}} = \frac{1}{nm}\sum_{i=1}^{n}\sum_{j=1}^{m}(P_{i,j} - m_{\mathrm{P}})^2 \tag{3}$$

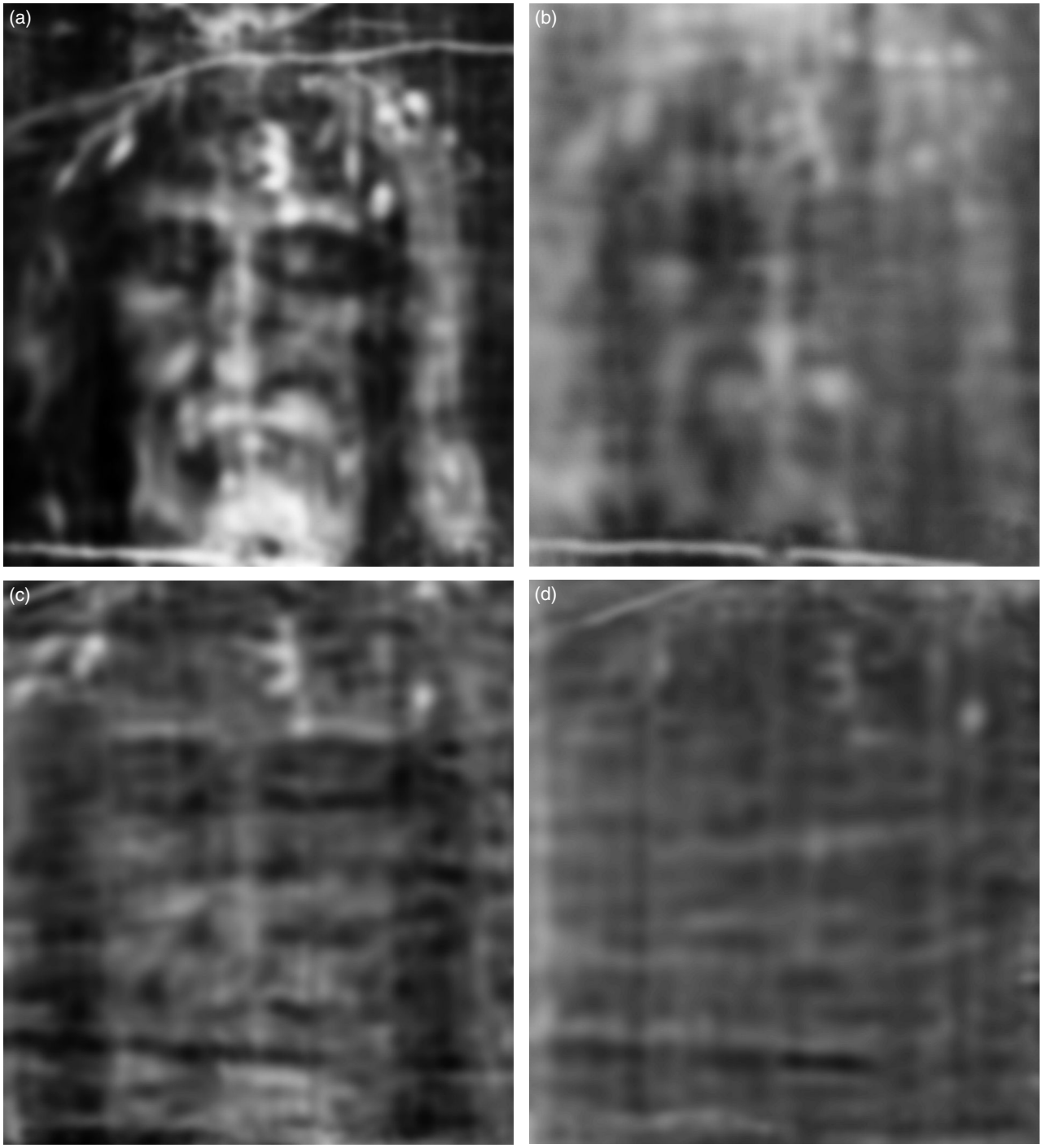

Figure 10. Processed photographs of the face: (a) visible light, fs (Enrie 1933); (b) IR (Judica Cordiglia 1976). (c) A face image, fs, visible light, directly acquired by scanning (Archdiocese 2000). (d) A face image, bs, visible light, directly acquired by scanning (Archdiocese 2000): although inferior in quality with respect to the result obtained by Ghiberti (2002), this image was used as a reference for the results.

and σ_{II} is the variance of the pixel value in the part of the image used for correlation:

$$\sigma_{\mathrm{II}} = \frac{1}{nm}\sum_{i=1}^{n}\sum_{j=1}^{m}(I_{i,j} - m_{\mathrm{I}})^2. \tag{4}$$

$I_{i,j}$ is the pixel value at position (i, j) in the image relative to the pattern position tested, $P_{i,j}$ is the pixel value at position (i, j) in the scaled and rotated pattern, m_{I} is the mean pixel value in the part of the image used for correlation:

$$m_{\mathrm{I}} = E(I_{i,j}) = \frac{1}{nm}\sum_{i=1}^{n}\sum_{j=1}^{m} I_{i,j}, \tag{5}$$

and m_{P} is the mean pixel value in the pattern:

$$m_{\mathrm{P}} = E(P_{i,j}) = \frac{1}{nm}\sum_{i=1}^{n}\sum_{j=1}^{m} P_{i,j}. \tag{6}$$

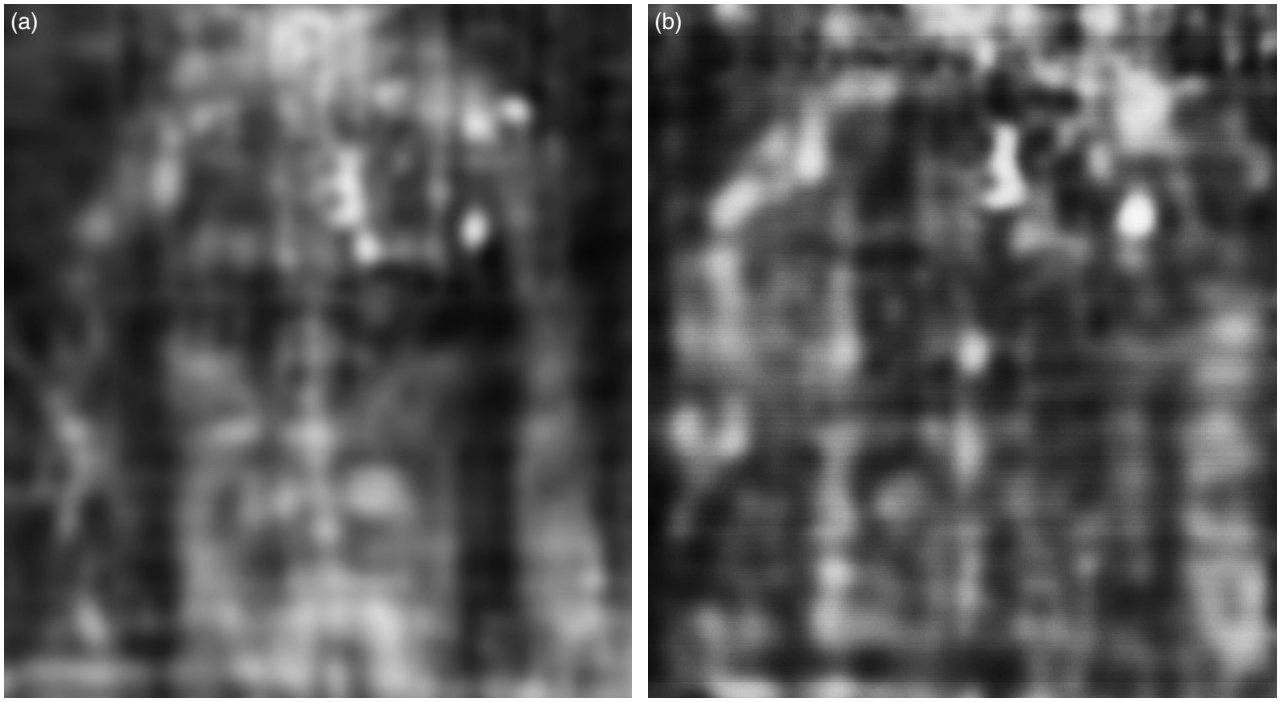

Figure 11. ((a), (b)) A processed face image, fs and bs (Ghiberti 2002), showing similar body features, comparison of which may help in understanding the mechanism of formation of the body image.

Table 1. Scores higher than 0.6 resulting from template matching of face images.

Score	(1) fs '02 bs '02	(2) fs '02 IR '69	(3) fs '02 Enrie	(4) bs '02 Enrie	(5) bs '02 IR '69	(6) bs '02 fs '02
(1) Moustache	0.69	0.74	0.88	0.61	0.71	0.72
(2) Nose tip	0.86	0.86	0.92	0.79	0.89	0.88
(3) Nose	0.80	0.92	0.88	0.77	0.82	0.79
(4) Eyes	0.61	0.65	0.89	—	—	—
(5) Hair, left	0.81	—	0.89	0.91	0.75	0.90
(6) Hair, right	—	—	0.65	0.64	—	—
(7) Eye, right	0.63	0.87	0.88	—	—	—
(8) Eye, left	—	—	0.96	—	0.72	0.61

In practice, a score of one is impossible to obtain, because of electro-optical noise in the digital image: this would mean perfect coincidence of the image, defined in the comparison window, with that of the template. A coefficient greater than 0.6 makes matching between the two images acceptable.

Comparisons were performed with reference to the following images:

(1) face, frontal image;
(2) arms and hands, frontal image;
(3) shoulders, dorsal image.

4.1. Face, frontal image

Comparisons were made with reference to the following details: (1) moustache and tip of the nose, (2) tip of the nose, (3) nose, (4) eyes, (5) detail of the hair, left, (6) detail of the hair, right, (7) eye, right, (8) eye, left.

Comparisons of the face images were made between the following processed images:

(1) fs (Ghiberti 2002) and bs (Ghiberti 2002);
(2) fs (Ghiberti 2002) and fs IR (Judica Cordiglia 1976);
(3) fs (Ghiberti 2002) and fs (Enrie 1933);
(4) bs (Ghiberti 2002) and fs (Enrie 1933);
(5) bs (Ghiberti 2002) and fs IR (Judica Cordiglia 1976);
(6) bs (Ghiberti 2002) and fs (Ghiberti 2002).

Note that the differences between comparisons (1) and (6) lie in the fact that, in comparisons (1)–(3), the template image is 'fs (Ghiberti 2002)', whereas in comparisons (4)–(6) it is 'bs (Ghiberti 2002)'. The resulting different scores depend on the type of template.

Table 1 shows the score results higher than 0.6 for different images and anatomical details. Comparisons with the images of the face, fs and bs (Archdiocese 2000), are not reported, because their quality, acquired with a scanner, is not comparable with that of the 2002 photographs. Although visually some anatomical details (hair, nose, eyes) can be recognized (Moran and Fanti 2002) in the face image, bs (Archdiocese 2000), template matching furnished relatively low scores. In any case, this image is important because it confirms, as a test of reproducibility, the body features highlighted in the image of the face, bs (Ghiberti 2002).

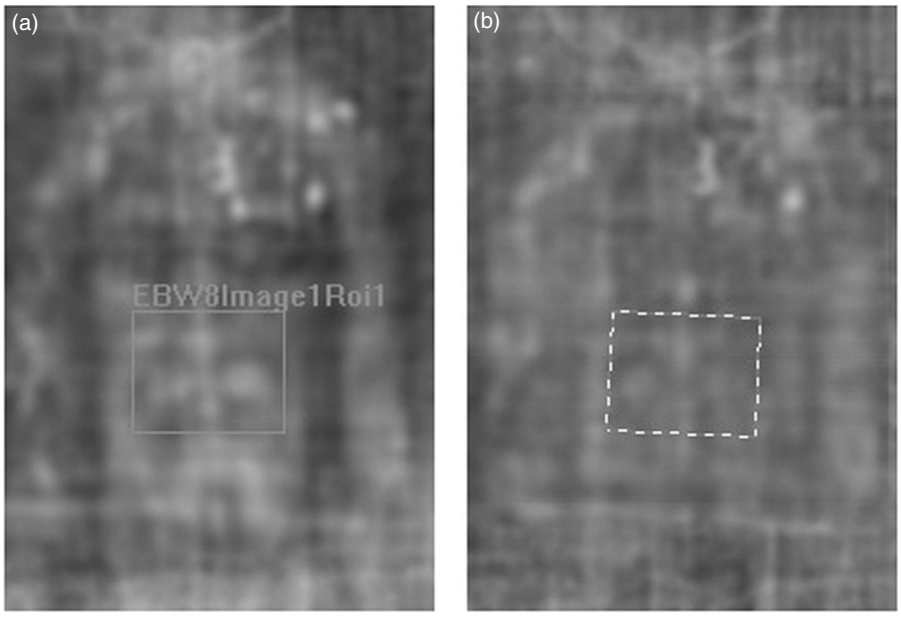

Figure 12. An example of the template matching application: (a) the template window corresponding to the nose and moustache on the face image, fs (Ghiberti 2002); (b) the detected window in the face image, bs (Ghiberti 2002), score 0.69.

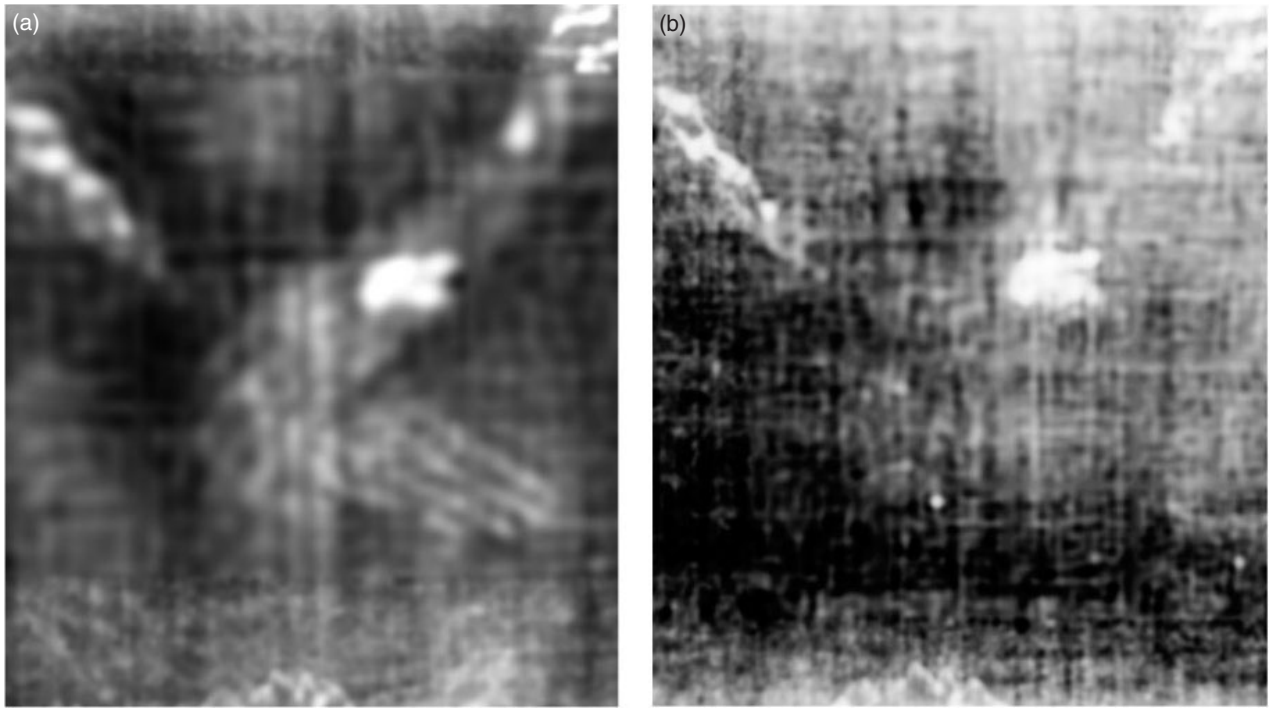

Figure 13. ((a), (b)) Processed images of the arms and hands, fs and bs (Ghiberti 2002). In (b), the resolution of image is insufficient to show fingers, but a clearer area in the centre, surrounded by a darker area, may be the imprint of hands.

Comparison of columns 1 and 6 reveals the stability of the results. In general, scores change by a few percentage points, but in some cases (e.g., eyes) the detail is recognized with a score of under 0.6. As regards column 3, the two different photographs of the same image furnish quite high scores, but none of them are equal to 1: they range from a maximum of 0.96 (right eye) to a minimum of 0.65 (hair to the right). Probably electro-optical noise, the difference in quality of the photographic films, and the different lighting conditions were responsible for these results.

Analysis of columns 1, 4, and 6 shows that the image of the face, bs (Ghiberti 2002), is recognized in all its detail as corresponding to the image of the face, fs: the hair, right side, is difficult to identify (only column 4), but it gave rise to other identification problems (see column 3). Recognition scores vary from 0.61 to 0.90, and it may therefore be stated that the features of the image of the face, bs, of the TS correspond to those of the face, fs. It should also be noted that the image of the face, bs, is found in the same position as the corresponding one on the front, in all its detail, and on the same scale, with non-

detectable relative rotation within the range of measurement uncertainty (3% for the scale factor, 3° for relative rotations).

The image of the face, fs, taken with IR film (columns 2 and 5) is not very similar to the corresponding photograph taken in visible light (column 3), because the maximum score does not exceed 0.92, but some details are not recognized (hair, left eye). Instead, a certain similarity of some details of the IR image with that of the bs can be observed: the tip of the nose, for example, gives a score of 0.89. Perhaps the characteristics of IR light in detecting in-depth details of the fabric contributed to producing an image similar to that of the bs.

Observe that the detail of the nose, bs, shows the best correspondence with the IR image (column 5, score 0.89) rather than with the image in visible light, fs (column 6, score 0.88).

As an example of the results, figure 12(a) shows the window corresponding to the details of the nose and moustache on the image of the face, fs (Ghiberti 2002), and figure 12(b) those of the face, bs (Ghiberti 2002) (score 0.88).

4.2. Arms and hands, frontal image

Recognizable details of arms and hands are not easy to find on the back image by means of the template matching technique, because details of fingers are not reproduced on the bs. Therefore, although it cannot objectively be stated that an image of the hands exists on the bs of the TS, the eye–brain system can perceive a clearer stain (figure 13(b)) which is correlated with the imprint of the hands (figure 13(a)).

Such an imprint on the bs of the TS does appear, although—for the time being—this cannot be shown numerically. If the Archdiocese in Turin makes available other photographs, including those taken in UV, which bring out details of the body image better in comparison with the background, it may be possible to verify that there is an imprint of the hands on the bs of the TS.

4.3. Shoulders, back image

Analysis of the back image focused on the shoulder area, because it is at that point that there is greater contrast between body features and the background. The procedure described in section 5 was applied to the bs image, but the resulting body image, if it exists, cannot be perceived either by numerical methods or by the human eye–brain system. If it does exist, it is masked by the noise of the digital image itself.

According to the quality of the images available up to now, traces of the back body image cannot be detected on the bs of the TS.

5. Characteristics of the face image on the back surface

The photograph of the face, bs, contains some body features such as the nose, eyes, hair, beard, and moustache, which show a face on the TS. This image is very similar to that of the face, fs (figure 11).

The image on the bs, like that on the fs, has the following properties. It presents as a photographic negative because the protruding parts are darker than the rest of the body (see section 2), but it is superficial because only the topmost fibres are involved in the dehydration characteristic of the image. It is a 3D image, as shown by Brice-4® (figure 14) and Optimas 6.1® processing (figures 15(a)–(d)).

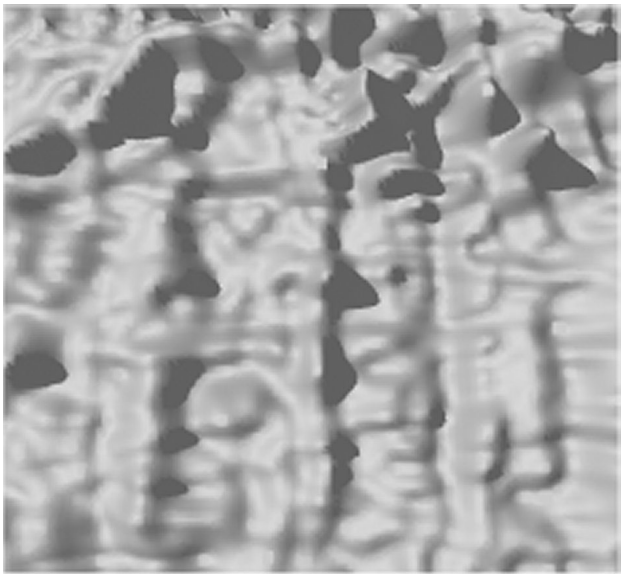

Figure 14. 3D processing of figure 11(b) with Brice-4® software. The right eye, tip of the nose, and moustache are evident.

It must be observed that the contribution of the image on the fs of the cloth to the image recorded on the bs of the cloth is practically nil. That is, the local optical penetration depth associated with producing each original photographic print and scanner data obtained directly from the cloth is less than the local fabric thickness. To show this, a thin layer of graphite (letters 'IL') was put on a piece of fabric having the same characteristics as the TS and it was photographed (both its front and back surface). As can be observed in figure 16, no signs appear on the bs.

This statement is strengthened if we observe that the image of the face impressed on the bs has some slight differences with respect to that on the fs. For example, the nose on the bs presents the same extension of both nostrils, unlike the fs, in which the right nostril is less evident (figures 11 and 15).

Since the body image on the fs is superficial (Weaver 1980, Pellicori and Evans 1981, Schwalbe and Rogers 1982, Jumper *et al* 1984, Jackson *et al* 1984, Adler 1999, Rogers 2002, 2003), and an image on the bs exists, the central part of the fabric was clearly not involved in the creation of the image—i.e., the internal part of the linen fabric does not have an image.

Therefore it has been ascertained that an image exists on the back of the TS. It certainly corresponds to the face and probably also to the hands, where the luminance levels are higher. In other words, there is an image on the bs corresponding with the one on the fs, which, at least as regards the face, corresponds to it in form, size, and position.

The face image is therefore doubly superficial. This means that, if a cross-section of the fabric is made, one extremely superficial image appears above and one below, but there is nothing in the middle (figure 17).

No image was detected on the bs corresponding to the dorsal image. If it exists, it is masked by digital noise.

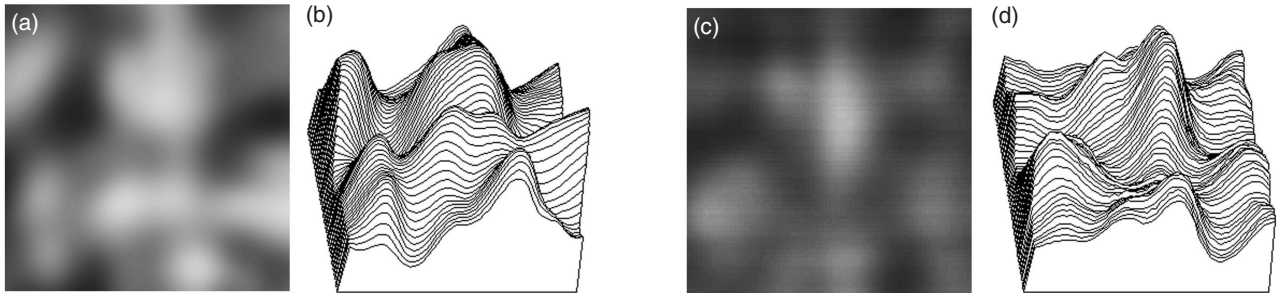

Figure 15. 3D processing of details of the nose and moustache with Optimas 6.1® software. ((a), (c)) Details of the processed images, fs and bs (Ghiberti 2002). ((b), (d)) 3D processing of images (a) and (c). Some differences in shape of the nose can be detected.

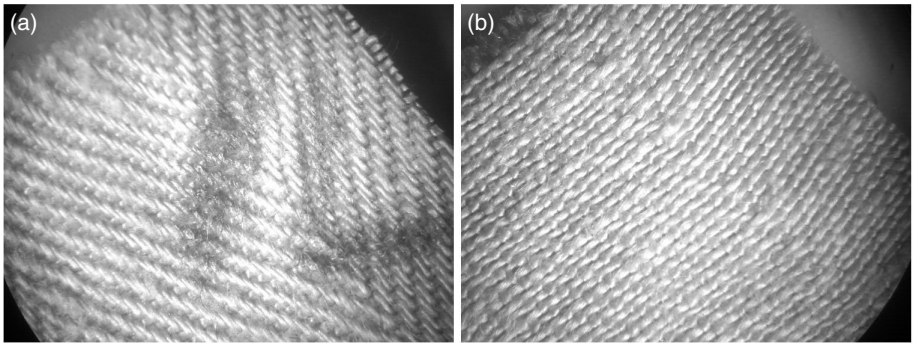

Figure 16. A photograph of a thin layer of graphite (letters 'IL') put on a piece of fabric having the same characteristics as the TS. (b) A high-contrast mirror image of its back surface; as no signs appear, the contribution of the image on the front surface of the cloth to the image recorded on the back surface of the cloth is practically nil.

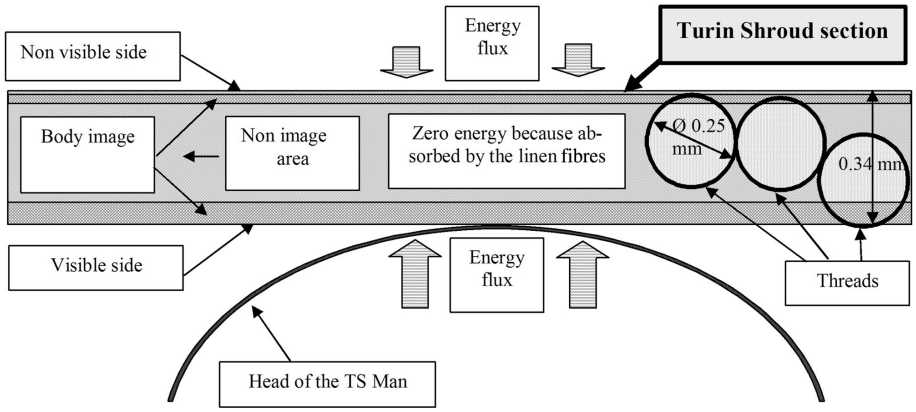

Figure 17. A sketch of a cross-section of the TS near the image of the face. Left: a section of sheet, 0.34 mm thick, showing body image and non-image areas; middle: a sketch of the possible source of energy creating the body image; right, the arrangement of fibres in the sheet, diameter 0.25 mm; only the topmost and bottommost parts of the threads show colouring corresponding to the body image.

Therefore, we only have the frontal image on the bs of the TS. This is what was postulated in earlier research (Jackson 1990), where however a hypothesis was made that is not yet scientifically verifiable, but the double superficiality is also explained by another phenomenon which may have been responsible for the formation of the body image: a corona discharge (Scheuermann 1983, 1984, Lattarulo 1998, De Liso 2002); future analyses will clarify this point.

6. Conclusions

This work analyses the first photographs of the back surface of the TS, made available by the Archdiocese of Turin. The double frontal and dorsal image of a man, imprinted on the front surface, is very faint. The body image on the bs is even fainter; i.e., the signal-to-noise ratio is about 0.5. For this reason, image processing was necessary to highlight body features, and an ad hoc image enhancement procedure was developed.

This procedure was based on convolution with Gaussian filters, summation of images to make the background more uniform, and filtering in spatial frequency by means of direct and inverse bidimensional FFTs. One limitation of this procedure would be revealed if both the images of interest and the defects were characterized by similar spatial frequency values, but this is not the case for the image of the TS man:

on the face, the spatial frequency values cover a field less than 100 m^{-1}, whereas the weft of the fabric, considered in this case as a defect, gives rise to spatial frequency values higher than 980 and 630 m^{-1} in the horizontal and vertical directions respectively.

The proposed method of enhancing digital images can be applied to a wide range of photographs that have deteriorated having spatial frequencies of the optical defects different from those of the image of interest.

Objective identification of body features was also performed by comparing images based on correlations furnished by template matching. It turns out that the face of the TS man is also present on the bs; the image of the hands is probably also partially visible on the bs, whereas no dorsal image (for example, the shoulders) can be detected.

As stated by many scientists, the body image is extremely superficial and gives rise to a particular characteristic: the double superficiality of the frontal image of the TS face. This characteristic will be taken into account in a future explanation of the body image formation mechanism.

References

Adler A D 1999 The nature of the body image on the Shroud of Turin *Proc. Shroud of Turin Int. Res. Conf. (Richmond, VA 1999)* ed B Walsh, in Crispino D (ed) 2002 *The Orphanated Manuscript* (Turin: Effata) pp 103–12

Archdiocese of Turin 2000 Sindone le immagini 2000 Shroud images (Torino, Italy: ODPF)

Basso R, Bianchini G and Fanti G 2002 Compatibilità fra immagine corporea digitalizzata e un manichino antropomorfo computerizzato *Proc. World Congress Sindone 2000 (Orvieto, Italy)* (San Servero: Gerni) pp 7–31

De Liso G 2002 Verifica Sperimentale della Formazione di Immagini su Teli Trattati con Aloe e Mirra in Concomitanza di Sismi *4th Int. Scientific Symp. on the Turin Shroud (Paris, April 2002)* (Paris: CIELT)

Enrie G 1933 *La Santa Sindone* (Turin: Società Editrice Internazionale) pp 47–51

Fanti G and Moroni M 2002 Comparison of luminance between face of the Turin Shroud man and experimental results *J. Imaging Sci. Technol.* **46-2** 142–54, Internet: http://www.imaging.org/store/epub.cfm?abstrid=8125

Ghiberti G 2002 *Sindone le Immagini 2002 Shroud Images* (Torino, Italy: ODPF)

Gilbert R Jr and Gilbert M 1980 Ultraviolet–visible reflectance and fluorescence spectra of the Shroud of Turin *Appl. Opt.* **19** 1930–6

Jackson J P 1990 Is the image on the Shroud due to a process heretofore unknown to modern science? *Shroud Spectr. Int.* **34** 3–29

Jackson J P, Jumper E J and Ercoline W R 1984 Correlation of image intensity on the Turin Shroud with the 3-D structure of a human body shape *Appl. Opt.* **23-14** 2244–70

Judica Cordiglia G B 1976 Come si è proceduto alla ripresa fotografica della SS. Sindone in occasione del 16 Giugno 1969, in Pellegrino M 1976 *Supplemento alla rivista Diocesana Torinese* (Turin: Centrostampa) pp 93–101

Jumper E J *et al* 1984 A comprehensive examination of the various stains and images on the Shroud of Turin *Archaeological Chemistry III* (*ACS Advances in Chemistry* vol 205–22) ed J B Lambert (Washington, DC: American Chemical Society) pp 447–76

Lattarulo F 1998 L'immagine sindonica spiegata attraverso un processo sismoelettrico *3rd Congresso Int. di Studi Sulla Sindone (Torino, Giugno 1998) Sindone e Scienza* CD-ROM (Turin: SATIZ)

Maggiolo R 2002/2003 Procedure eidomatiche... *Degree Thesis* Dipartimento di Ingegneria Meccanica, University of Padova (tutor G Fanti) (http://www.shroud.com/group/facereverse.jpg)

Marion A 1998 Discovery of inscriptions on the shroud of Turin *Opt. Eng.* **37/38** 2308–13

Miller V D and Pellicori S F 1981 Ultraviolet fluorescence photography of the Shroud of Turin *J. Biol. Photography* **49** (3) 71–85

Moran K and Fanti G 2002 Does the Shroud body image show any physical evidence of Resurrection? *4th Int. Scientific Symp., Centre Int. d'Études sur le Linceul de Turin (Paris, April 2002)* (Paris: CIELT)

Pellicori S and Evans M S 1981 The Shroud of Turin through the microscope *Archaeology* **34** 34–43

Rogers R 2002 *Scientific Method Applied to the Shroud of Turin, a Review* http://shroud.com/pdfs/rogers2.pdf

Rogers R 2003 personal communication to G Fanti

Scheuermann O 1983 *Hypothesis: Electron Emission or Absorption as the Mechanism that Created the Image on the Shroud of Turin—Proof by Experiment* 1st edn Archive of Fondazione 3M (Milan: Segrate)

Scheuermann O 1984 *Appendix I to Hypothesis: Electron Emission or Absorption as the Mechanism that Created the Image on the Shroud of Turin—Proof by Experiment* (personal communication to G Fanti 2003)

Schwalbe L A and Rogers R N 1982 Physics and chemistry of the Shroud of Turin, a summary of the 1978 investigations *Anal. Chim. Acta* **135** 3–49

Schwortz B M 1982 Mapping of research test-point areas on the Shroud of Turin *Proc. IEEE Int. Conf. on Cybernetics and Society* (Piscataway, NJ: IEEE) pp 538–47

Weaver K F 1980 Science seeks to solve... The mystery of the Shroud *National Geographic* **157** 741